frontiers in Chemistry

ORIGINAL RESEARCH
published: 28 January 2019
doi: 10.3389/fchem.2019.00017

# Highly Efficient Thermally Activated Delayed Fluorescence Emitter Developed by Replacing Carbazole With 1,3,6,8-Tetramethyl-Carbazole

*Jia-Lin Cai[1], Wei Liu[2], Kai Wang[2], Jia-Xiong Chen[2], Yi-Zhong Shi[2], Ming Zhang[1], Cai-Jun Zheng[1]*, Si-Lu Tao[1]* and Xiao-Hong Zhang[2]**

[1] School of Optoelectronic Science and Engineering, University of Electronic Science and Technology of China, Chengdu, China, [2] Institute of Functional Nano and Soft Materials, Jiangsu Key Laboratory for Carbon-Based Functional Materials and Devices, Soochow University, Suzhou, China

Carbazole (Cz) is the one of the most popular electron donors to develop thermally activated delayed fluorescence (TADF) emitters, but additional groups are generally required in the molecules to enhance the steric hindrance between Cz and electron acceptor segments. To address this issue, we replaced Cz with its derivative 1,3,6,8-tetramethyl-carbazole (tMCz) to develop TADF emitters. Two novel compounds, 6-(4-(carbazol-9-yl)phenyl)-2,4-diphenylnicotinonitrile (CzPN) and 2,4-diphenyl-6-(4- (1,3,6,8-tetramethyl-carbazol-9-yl)phenyl) nicotinonitrile (tMCzPN) were designed and synthesized accordingly. With the same and simple molecular framework, tMCzPN successfully exhibits TADF behavior, while CzPN is a non-TADF fluorophor, as the additional steric hindrance of methyl groups leads to a more twisted structure of tMCzPN. In the organic light-emitting diodes (OLEDs), tMCzPN exhibits extremely high forward-viewing maximum external quantum efficiency of 26.0%, without any light out-coupling enhancement, which is significantly higher than that of 5.3% for CzPN. These results indicate that tMCzPN is an excellent TADF emitter and proves that tMCz is a more appropriate candidate than Cz to develop TADF emitters.

**Keywords: thermally activated delayed fluorescence, steric hindrance, OLED, 1, 3, 6, 8-tetramethyl-carbazole, dihedral angle**

OPEN ACCESS

***Edited by:***
*Shi-Jian Su,*
*South China University of Technology, China*

***Reviewed by:***
*Qisheng Zhang,*
*Zhejiang University, China*
*Chuluo Yang,*
*Wuhan University, China*

***Correspondence:**
*Cai-Jun Zheng*
*zhengcaijun@uestc.edu.cn*
*Si-Lu Tao*
*silutao@uestc.edu.cn*
*Xiao-Hong Zhang*
*xiaohong_zhang@suda.edu.cn*

***Specialty section:***
*This article was submitted to Organic Chemistry, a section of the journal Frontiers in Chemistry*

***Received:*** *16 November 2018*
***Accepted:*** *08 January 2019*
***Published:*** *28 January 2019*

***Citation:***
*Cai J-L, Liu W, Wang K, Chen J-X, Shi Y-Z, Zhang M, Zheng C-J, Tao S-L and Zhang X-H (2019) Highly Efficient Thermally Activated Delayed Fluorescence Emitter Developed by Replacing Carbazole With 1,3,6,8-Tetramethyl-Carbazole. Front. Chem. 7:17. doi: 10.3389/fchem.2019.00017*

## INTRODUCTION

Organic light-emitting diodes (OLEDs) have attracted great attention and are considered as next-generation solid-state lighting and displays because of their flexibility, light weight, and low-cost fabrication (Pope et al., 1963; Tang and VanSlyke, 1987; Baldo et al., 1998; Goushi et al., 2012; Uoyama et al., 2012; Zheng et al., 2013; Liu et al., 2015b,c; Li et al., 2018; Shi et al., 2018). Based on spin quantum statistics, electrical excitation generates 25% singlet excitons and 75% triplet excitons in the devices (Segal et al., 2003). OLEDs based on traditional fluorescent emitters can only utilize singlet excitons with a maximum internal quantum efficiency (IQE) of 25% (Baldo et al., 1999; Segal et al., 2003). To harvest triplet excitons, phosphorescent OLEDs, using heavy metal complexes as emitters, were developed, and successfully realized with 100% IQE, due to the strong spin-orbit coupling effect of heavy metal irons (Baldo et al., 1998; Adachi et al., 2001; Sajoto et al., 2009; Yersin et al., 2011). However, noble metal complexes also lead to expensive costs and environmental hazards, which further constrains the development of phosphorescent OLEDs (Méhes et al., 2012; Zhang et al., 2014c, 2015).

To address this issue, Adachi and co-workers firstly introduced pure organic molecules with thermally activated delayed fluorescence (TADF) characteristic as emitters for OLEDs (Uoyama et al., 2012). TADF emitters can convert non-radiative triplet excitons to radiative singlet excitons through an efficient reverse intersystem crossing (RISC) process, thus TADF-based OLEDs can also theoretically achieve 100% IQE (Endo et al., 2009). As a TADF emitter, it is key to realize an extremely small singlet and triplet energy splitting ($\Delta E_{ST}$) for an efficient RISC process (Peng et al., 2013). Therefore, nearly all reported TADF emitters were developed by connecting electron-donor (D) and electron-acceptor (A) segments with a highly twisted structure (Zhang et al., 2014a, 2017; Liu et al., 2016; Chen et al., 2017; Wang et al., 2017), as such a highly twisted D-A molecular framework can naturally separate the highest occupied molecular orbital (HOMO) and lowest unoccupied molecular orbital (LUMO) on the D and A segments respectively, which is the general requirement for extremely small $\Delta E_{ST}$s (Endo et al., 2011; Zhang et al., 2012, 2014a,b). Among the reported TADF emitters, carbazole (Cz) is one of the most popular D candidates due to its planar aromaticity, appropriate energy levels, feasible modification and good chemical stability (Uoyama et al., 2012; Liu et al., 2015a; Mounggon et al., 2015; Chan et al., 2018; Pashazadeh et al., 2018). However, with the relatively small steric hindrance of the Cz segment, Cz-A structure TADF emitters usually possess moderate dihedral angles between the Cz and A segments around 45° (Hirata et al., 2014; Zhang et al., 2018), which induces higher $\Delta E_{ST}$s and hinders the RISC process. Thus, to develop Cz-A structure TADF emitters, additional groups are generally required to enhance the steric hindrance between the Cz and A segments, which lead to complicated synthetic procedures and high costs.

To address this issue, Cz's derivative group 1,3,6,8-tetramethyl-carbazole (tMCz) has been proposed to replace the Cz group in the development of TADF emitters. Compared with Cz, the methyl groups at 1, 8 positions on tMCz can enhance the steric hindrance between tMCz and A segments, thus leading to more twisted structures of the compounds without other additional groups. In 2017, Adachi and co-workers developed a TADF emitter Cz-TRZ2 with tMCz group and realized a maximum EQE of 22.0% in the OLED (Cui et al., 2017). In this work, we designed and synthesized two novel compounds 6-(4-(carbazol-9-yl)phenyl)-2,4-diphenylnicotinonitrile (CzPN) and 2,4-diphenyl-6-(4-(1,3,6,8-tetramethyl-carbazol-9-yl)phenyl) nicotinonitrile (tMCzPN) by combining Cz or tMCz with electron-acceptor diphenylnicotinonitrile (Liu et al., 2015a), in a simple molecular framework. With the same molecular framework, the dihedral angles between the Cz (or tMCz) and phenylnicotinonitrile segments are 52° for CzPN and 84.9° for tMCzPN, respectively, proving that tMCz can better separate the HOMO and LUMO than Cz can. Moreover, tMCzPN successfully exhibits TADF characteristic with a small $\Delta E_{ST}$ of 0.10 eV, while CzPN is a non-TADF fluorophor with a large $\Delta E_{ST}$ of 0.32 eV. In these devices, CzPN exhibits low forward-viewing maximum current efficiency (CE), power efficiency (PE), and external quantum efficiency (EQE) of 4.7 cd $A^{-}$ (Pope et al., 1963), 4.7 lm $W^{-1}$, and 5.3%, respectively, consistent with common traditional fluorescent emitters. Additionally, the tMCzPN-based OLED shows high forward-viewing maximum efficiencies of 26.0% for EQE, 65.9 cd $A^{-1}$ for CE, and 62.7 lm $W^{-1}$ for PE, without any light out-coupling enhancement. To the best of our knowledge, these high efficiencies are among the best reported TADF-based OLEDs, proving that tMCz is a more appropriate candidate than Cz to develop TADF emitters.

# EXPERIMENTAL

## General Methods

$^{1}H$ nuclear magnetic resonance (NMR) and $^{13}C$ NMR spectral data were obtained by using an AVANCZ spectrometer. Mass spectral (MS) data were measured using a Finnigan 4021C gas chromatography mass spectrometry instrument. Absorption and Photoluminescence (PL) spectra were obtained using a Hitachi UV-vis spectrophotometer U-3010 and a Hitachi fluorescence spectrometer F-4600, respectively. Cyclic voltammetry (CV) measurements were performed using a CHI660E electrochemical analyzer, while the oxidation potential of saturated calomel electrode (SCE) relative to the vacuum level is calibrated to be 4.56 eV in dimethylformamide (DMF). Transient PL spectra were obtained using Edinburgh Instruments FLS980 spectrometer. The photoluminescence quantum yields (PLQYs) of mixed DPEPO (bis[2-(di-(phenyl)phosphino)-phenyl]ether oxide) solid films were investigated using a QY-2000 fluorescence spectrometer and estimated via a F-3018 Integrating Sphere. Thermogravimetric analysis (TGA) and differential scanning calorimetry (DSC) measurements were performed using a TAQ 500 thermogravimeter and a NETZSCH DSC204 instrument in $N_2$, respectively.

## Synthesis

The commercially available reagents and materials were used directly without purification.

### (E)-1-(4-bromophenyl)-3-phenylprop-2-en-1-one

A mixture of 1-(4-bromophenyl)ethan-1-one (2.0 g, 10 mmol) and benzaldehyde (2.12 g, 20 mmol) was stirred in 20 ml of ethanol and a 10% NaOH solution for 30 min at room temperature. The reaction mixture was allowed to stand for 1 h and then filtered and recrystallized from ethanol to obtain a light yellow powder (E)-1-(4-bromophenyl)-3-phenylprop-2-en-1-one (2.5 g, 87% yield). The crude product was dried in a vacuum oven directly for the next step.

### 6-(4-bromophenyl)-2,4-diphenylnicotinonitrile

3-oxo-3-phenylpropanenitrile (1.45 g, 10 mmol), (E)-1-(4-bromophenyl)-3-phenylprop-2-en-1-one (2.87 g, 10 mmol) and anhydrous ammonium acetate (4.01 g, 52 mmol) was dissolved in glacial acid (8 mL). The mixture was refluxed under stirring for 2 h at 110°C. After cooling to room temperature, the reaction was neutralized using a 10% NaOH solution and extracted with dichloromethane. The dichloromethane phase was then dried with anhydrous sodium sulfate. After evaporation of

the solvent, the crude product was purified through silica gel column chromatography, using 1:3 dichloromethane/petroleum as eluent to obtain a white solid powder 6-(4-bromophenyl)-2,4-diphenylnicotinonitrile (1.0 g, 24.3% yield). $^1$H NMR (600 MHz, Chloroform-*d*) δ 8.09–8.00 (m, 4H), 7.79 (s, 1H), 7.73 – 7.61 (m, 4H), 7.56 (dt, $J$ = 7.7, 5.8 Hz, 6H). $^{13}$C NMR (151 MHz, Chloroform-*d*) δ 162.62, 158.05, 155.80, 137.95, 136.74, 136.51, 132.32, 130.32, 130.16, 129.48, 129.18, 128.79, 128.69, 125.43, 118.50, 117.70, 104.81. MS (EI) m/z: [M]+ calcd for $C_{24}H_{15}BrN_2$, 411.30; found, 411.05.

## 6-(4-(Carbazol-9-yl)phenyl)-2,4-diphenylnicotinonitrile (CzPN)

A mixture of 6-(4-bromophenyl)-2,4-diphenylnicotinonitrile (0.411 g, 1 mmol), Cz (0.200 g, 1.2 mmol), sodium tert-butoxide (0.192 g, 2 mmol), tris(dibenzylideneacetone)dipalladium (0.018 g, 0.02 mmol) and tri-tert-butylphosphine tetrafluoroborate (0.023 g, 0.008 mmol) was added into toluene (10 mL) under $N_2$ and then refluxed at 110°C for 12 h. After cooling to room temperature, the mixture was filtered with diatomite. The solvent of the filtrate was removed under reduced pressure. The crude product was purified through silica gel column chromatography, using 1:3 dichloromethane/petroleum as eluent to obtain a green solid powder (0.425g, 86% yield). $^1$H NMR (600 MHz, Chloroform-*d*) δ 8.45 – 8.42 (m, 2H), 8.16 (d, $J$ = 7.7 Hz, 2H), 8.11 – 8.07 (m, 2H), 7.92 (d, $J$ = 1.6 Hz, 1H), 7.75 (ddd, $J$ = 11.0, 7.5, 1.7 Hz, 4H), 7.63 – 7.54 (m, 6H), 7.51 (d, $J$ = 8.2 Hz, 2H), 7.46 – 7.42 (m, 2H), 7.32 (t, $J$ = 7.4 Hz, 2H). $^{13}$C NMR (151 MHz, Chloroform-*d*) δ 162.56, 158.15, 155.66, 140.44, 139.83, 137.88, 136.66, 136.27, 130.17, 130.02, 129.36, 129.11, 129.04, 128.67, 128.56, 127.17, 126.09, 123.64, 120.41, 120.32, 118.61, 117.62, 109.76, 104.55. MS (EI) m/z: [M]+ calcd for $C_{36}H_{23}N_3$, 497.60; found, 497.19.

## 2,4-diphenyl-6-(4-(1,3,6,8-tetramethyl-carbazol-9-yl)phenyl)nicotinonitrile (tMCzPN)

tMCzPN was synthesized according to the same procedure as CZN,by using tMCz instead of Cz. After cooling to room temperature, the mixture was filtered with diatomite. The solvent of filtrate was removed under reduced pressure; the crude product was purified through silica gel column chromatography using 1:3 dichloromethane/petroleum as eluent to obtain a yellow solid powder (0.25 g, 45% yield). $^1$H NMR (600 MHz, Chloroform-*d*) δ 8.32 (d, $J$ = 8.4 Hz, 2H), 8.08 (dd, $J$ = 8.0, 1.6 Hz, 2H), 7.95 (s, 1H), 7.80–7.69 (m, 4H), 7.66 – 7.53 (m, 8H), 6.92 (s, 2H), 2.48 (s, 6H), 1.93 (s, 6H). $^{13}$C NMR (151 MHz, Chloroform-*d*) δ 162.75, 158.04, 155.92, 144.86, 139.51, 138.07, 137.75, 136.85, 132.03, 130.46, 130.44, 130.25, 129.58, 129.36, 129.26, 128.87, 128.82, 127.52, 124.45, 121.36, 118.98, 118.05, 117.78, 104.95, 21.32, 19.82. MS (EI) m/z: [M]+ calcd for $C_{40}H_{31}N_3$, 553.71; found, 553.25.

## Device Fabrication and Measurements

ITO-coated glass substrates with a sheet resistance of 30 Ω per square, were cleaned with acetone and ethanol, then washed with deionized water for 5 min, and then oven-dried at 120°C and treated with UV-ozone for 5 min. The cleaned substrates were then moved into the vacuum evaporation chamber. The

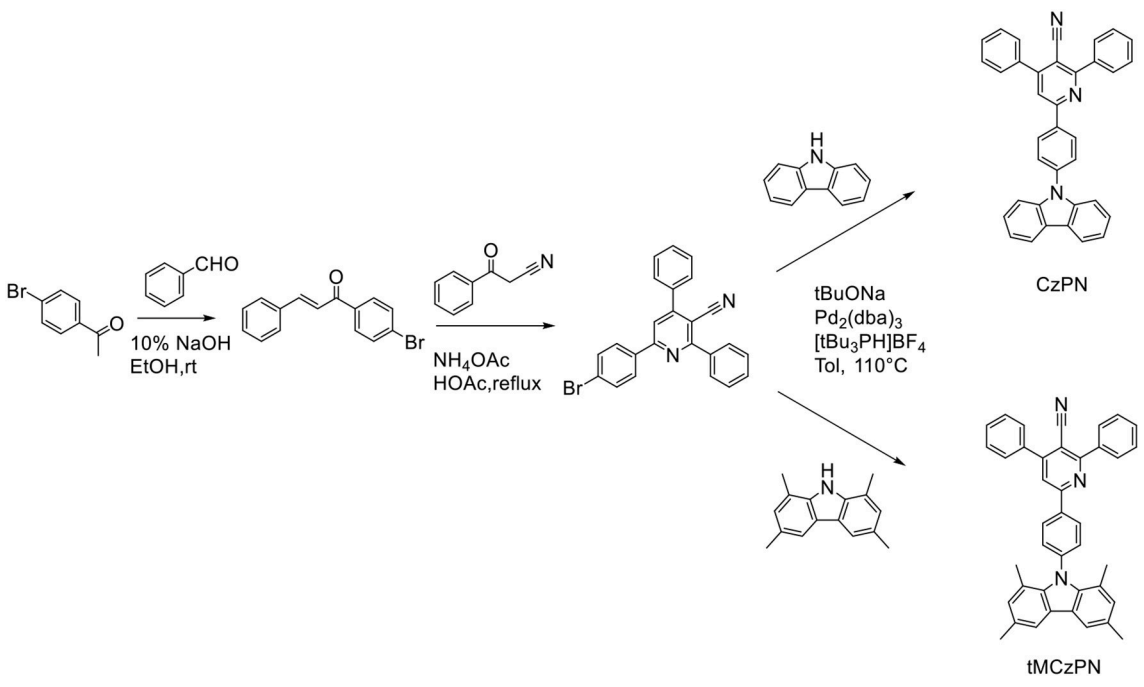


**SCHEME 1 |** Synthetic routes and molecular structures of CzPN and tMCzPN.

organic layers were deposited onto the substrates through thermal evaporation under $1 \times 10^{-6}$ Torr with the rate of 1–2 Å $s^{-1}$. The rate was 0.1 Å $s^{-1}$ for LiF, and 10 Å $s^{-1}$ for Al. The electroluminescence (EL) spectra and CIE color coordinates were measured using a Spectrascan PR650 instrument. The current density-voltage characteristics were obtained using a Keithley 2400 Source Meter controlled by a computer. The EQE was calculated from the current density, luminance, and EL

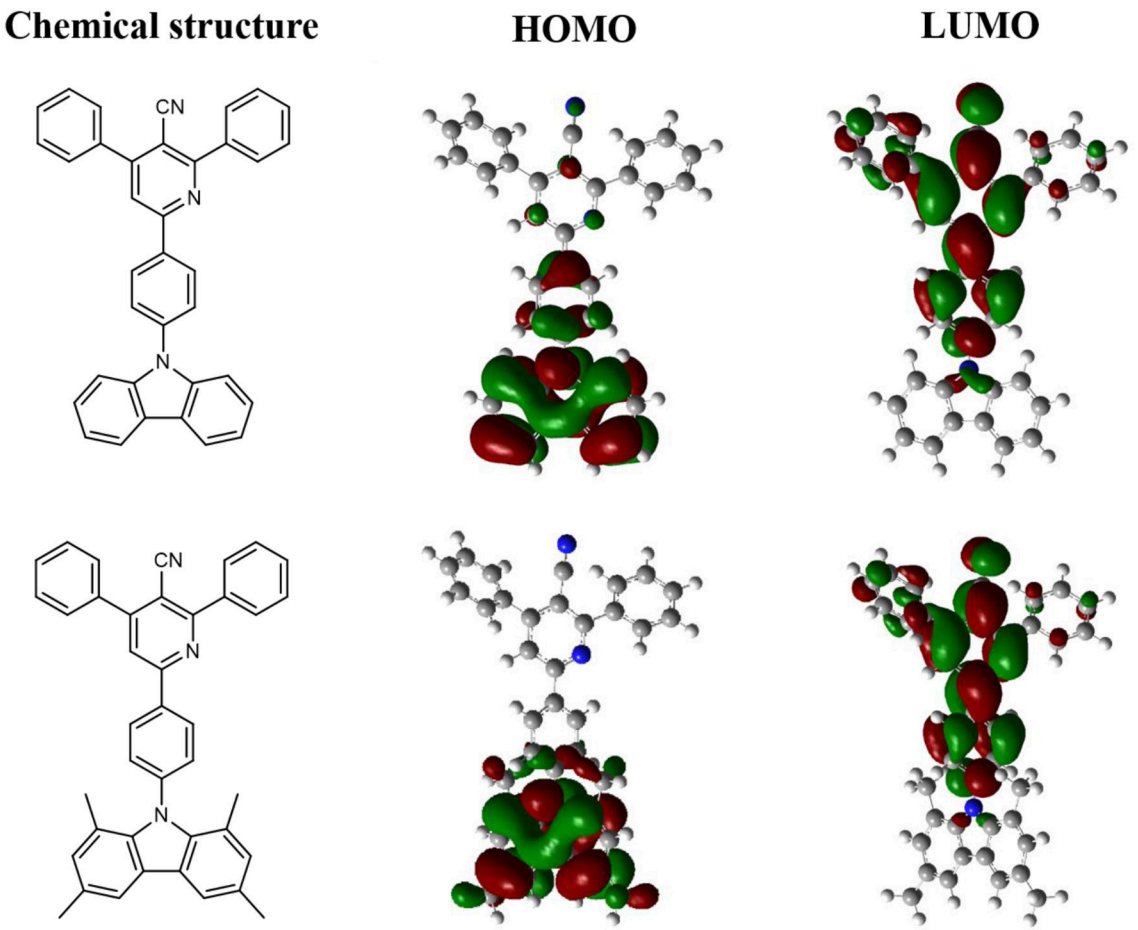


**FIGURE 1 |** Chemical structures, HOMO and LUMO distributions of CzPN and tMCzPN.

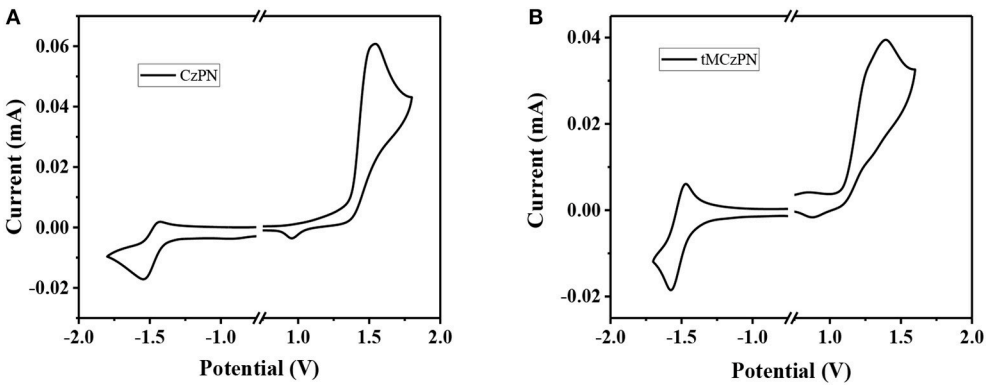


**FIGURE 2 |** Cyclic voltammograms of **(A)** CzPN and **(B)** tMCzPN in DMF recorded with a scan rate of 0.05 V/s. The HOMO and LUMO levels are calculated with the equation: HOMO $= -e(E_{ox} + 4.56)$, LUMO $= -e(E_{red} + 4.56)$. $E_{ox}$, $E_{red}$ are the onsets of oxidation and reduction curves.

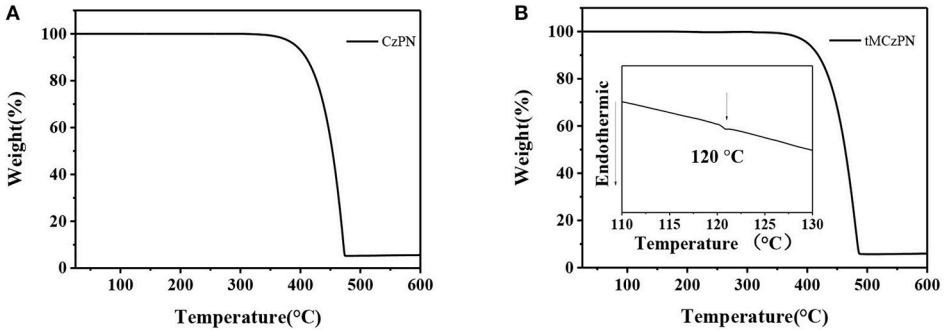


**FIGURE 3 |** TGA and DSC measurements of **(A)** CzPN and **(B)** tMCzPN recorded with a heating rate of 10°C/min.

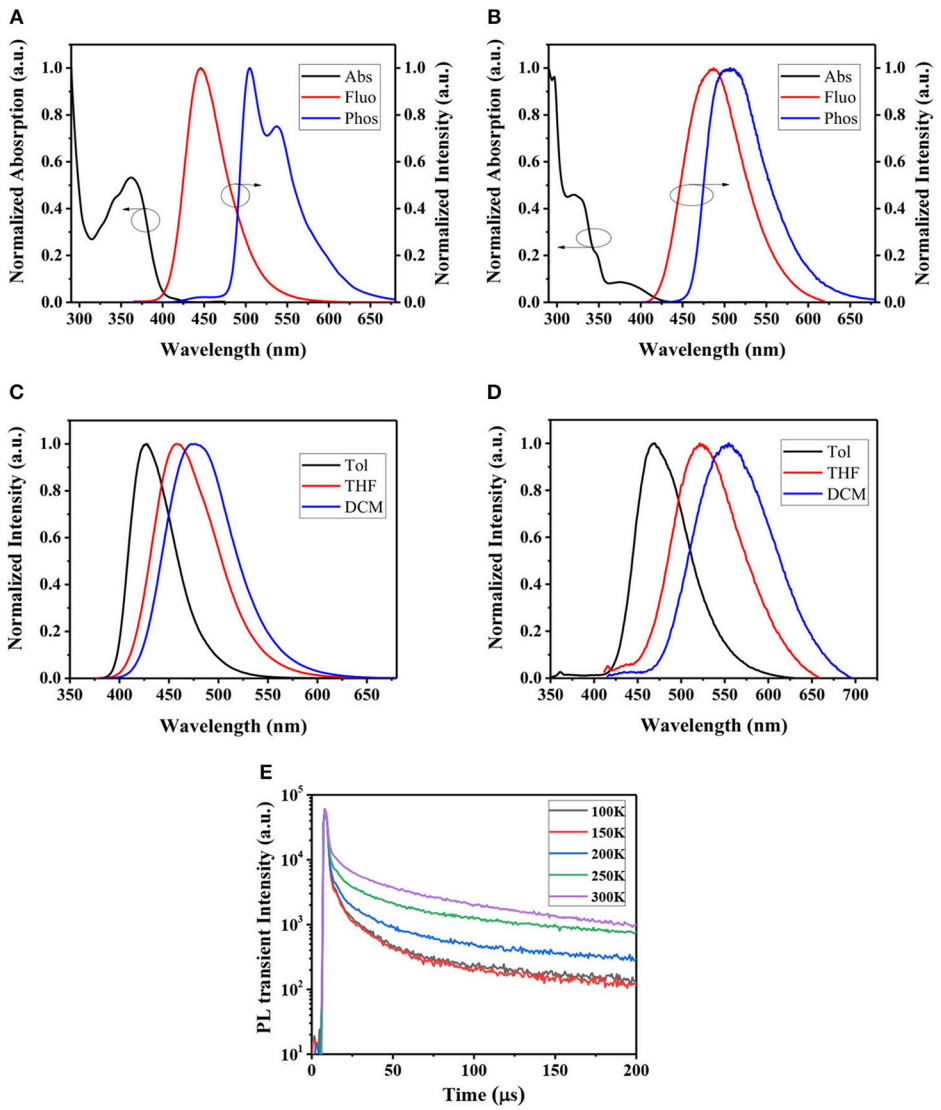


**FIGURE 4 |** UV-Vis absorption spectra in toluene, fluorescence spectrum in DPEPO film at room temperature, and phosphorescence spectra in DPEPO film at 77K of **(A)** CzPN and **(B)** tMCzPN. Fluorescence spectra of **(C)** CzPN and **(D)** tMCzPN in different solvent (Tol, toluene; DCM, dichloromethane; and THF, tetrahydrofuran). **(E)** Temperature-dependent transient PL decay spectra of tMCzPN doped in DPEPO film by exciting at 300 nm (20 wt.%).

spectrum, assuming a Lambertian distribution (Okamoto et al., 2001).

# RESULTS AND DISCUSSION

## Synthesis

As shown in **Scheme 1**, both two compounds were synthesized through three steps. The (E)-1-(4-bromophenyl)-3-phenylprop-2-en-1-one was synthesized by aldol reaction between benzaldehyde and 1-(4-bromophenyl)ethan-1-one. And the cyanopyridine derivative was synthesized by cyclizing a pyridine ring between 3-oxo-3-phenylpropanenitrile and (E)-1-(4-bromophenyl)-3-phenylprop-2-en-1-one with ammonium acetate as the source of nitrogen. Then, the final products were synthesized through the Buchwald-Hartwig coupling reaction between cyanopyridine derivative and the corresponding Cz derivatives. The chemical structure of CzPN and tMCzPN were characterized and confirmed by $^{1}$H NMR and $^{13}$C NMR spectroscopies and mass spectrometry. Moreover, CzPN and tMCzPN were purified by sublimation before further characterizations.

## Theoretical Calculations and Electrochemical Properties

To analyze the relationships between the structures and properties of CzPN and tMCzPN at the molecular level, we performed the density function theory (DFT) calculation for both compounds at the B3LYP/6-31G(d) level. The optimized ground-state conformations and HOMO and LUMO distributions of the two compounds are shown in **Figure 1**. In the CzPN molecule, the dihedral angle between the Cz and phenylnicotinonitrile segments was optimized to 52°, which is close to other reported common Cz-A structure compounds, without steric hindrance between the D and A segments (Choi et al., 2017; Rajamalli et al., 2017; Liang et al., 2018) . Caused by such insufficient twist, both the HOMO and LUMO of CzPN are extended to the central benzene bridge. The obvious overlap between HOMO and LUMO leads to an evident conjugation and a large $\Delta E_{ST}$ for CzPN, which suppresses the TADF behavior. Reversely, due to the large hindrance of the two methyl groups at 1, 8 positions on the Cz, tMCzPN possesses a nearly vertical dihedral angle between the Cz and phenylnicotinonitrile segments of 84.9°. The HOMO is mainly confined on the tMCz segment and the LUMO is located on the phenylnicotinonitrile unit, realizing a nearly full separation between HOMO and LUMO. Thus, by replacing Cz with tMCz, tMCzPN successfully possesses a more twisted molecular structure and is predicted to have an extremely small $\Delta E_{ST}$ and the TADF characteristic theoretically.

We further investigated the electrochemical properties of both compounds by CV in DMF. As shown in **Figure 2**, from the onsets of oxidation curves, the HOMO energy levels of CzPN and tMCzPN are estimated to be −5.93 and −5.66 eV, respectively. As the electron-donating ability of the four methyl groups, tMCz has a much higher HOMO energy level than Cz. Whereas, from the onsets of reduction curves, the LUMO energy levels of CzPN and tMCzPN are calculated to be of similar values of −3.16 and −3.13 eV, respectively.

## Thermal Properties

The thermal properties of CzPN and tMCzPN were characterized by TGA and DSC measurements under a nitrogen atmosphere. As shown in **Figure 3**, two compounds exhibit high decomposition temperatures ($T_d$s) (corresponding to 5.0 % weight loss) of 392°C for CzPN and 400°C for tMCzPN, respectively, suggesting that both are capable of vacuum purification and evaporation. The glass transition temperature ($T_g$) of tMCzPN is determined to be 120°C, and no glass transition was observed for CzPN from 25 to 250°C. The high $T_g$ of tMCzPN would be beneficial to its morphological stability and reduce the phase separation rate of the guest-host system.

## Photophysical Properties

Room temperature UV-Vis absorption spectra of CzPN and tMCzPN in toluene are shown in **Figure 4**. At the long-wavelength region, both compounds show broad absorption bands with peaks at 362 and 375 nm, respectively for CzPN, and tMCzwhich are assigned to the intramolecular charge transfer (ICT) transition from the electron donor Cz to the electron acceptor phenylnicotinonitrile. Additionally, the ICT absorption of tMCzPN was much weaker than that of CzPN, which is ascribed to its better separation between the HOMO and LUMO as shown in **Figure 2**. With the ICT transition characteristic, both compounds exhibit obvious solvatochromic effects in variated solvents as shown in **Figures 4C,D**. From low-polar toluene to high-polar dichloromethane, the emission peak of CzPN is red-shifted from 427 to 477 nm, while the emission peak of tMCzPN is red-shifted from 468 to 554 nm. As the solvatochromic effect is related to structure relaxation of the ICT molecule, CzPN, which has a higher molecular restriction due to stronger conjugation between the D and A segments, exhibits a much weaker red-shift compared to tMCzPN accordingly.

The PL spectra of the two compounds doped in DPEPO films were further studied. At room temperature, CzPN and

**TABLE 1 |** Key physical properties of two compounds.

| Compounds | $\lambda_{abs}$ (nm) [a] | $\lambda_{fluo}$ (nm) [b] | $\lambda_{phos}$ (nm) [c] | $\Delta E_{ST}$ (eV) [d] | HOMO (eV) [e] | LUMO (eV) [f] | $T_d/T_g$ (°C) | PLQY (%) |
|---|---|---|---|---|---|---|---|---|
| CzPN | 362 | 446 | 505 | 0.32 | −5.93 | −3.16 | 392/ | 93.3 |
| tMCzPN | 375 | 487 | 507 | 0.10 | −5.66 | −3.13 | 400/120 | 70.5 |

*[a]Measured in toluene solution at room temperature. [b]Measured in DPEPO film at room temperature. [c]Measured in DPEPO film at 77 K. [d]Estimated from the peak of fluorescence and phosphorescence spectra. [e]Calculated from the onset of oxidation potential. [f]Calculated from the onset of reduction potential.*

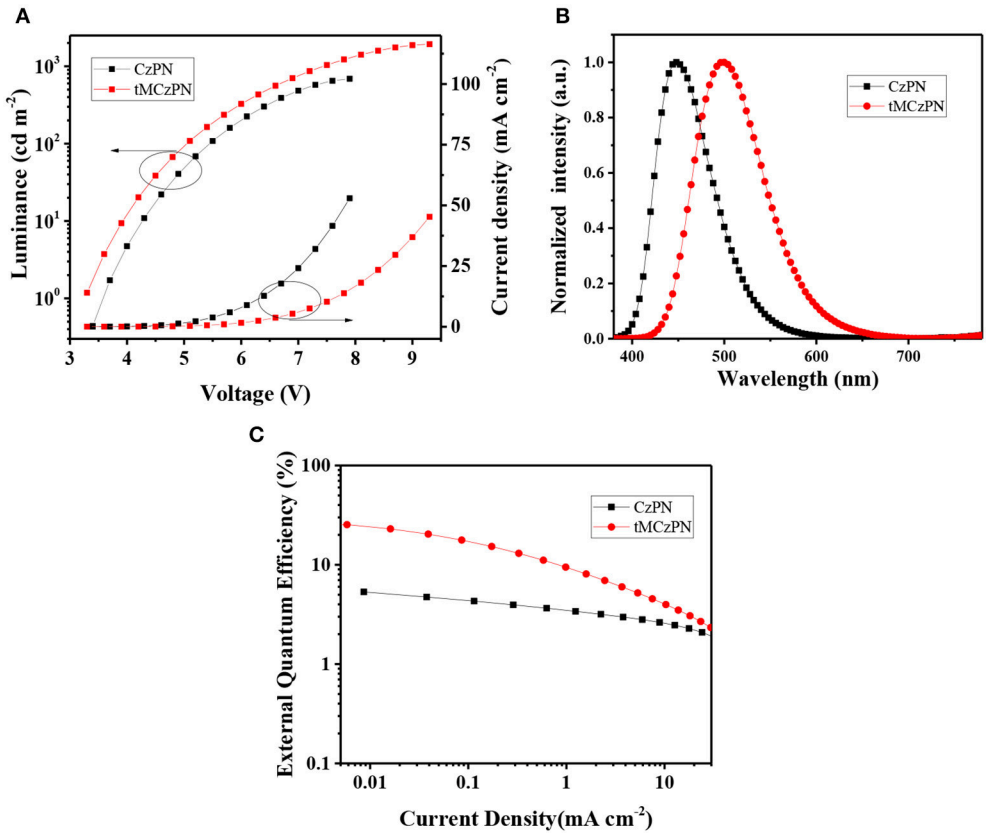


**FIGURE 5 | (A)** Current density-voltage-luminance characteristics, **(B)** EL spectra, and **(C)** Current density-EQE characteristics of the devices based on CzPN and tMCzPN.

**TABLE 2 |** Electroluminescence properties of the devices.

| Emitters | $V_{on}$ (V)[a] | $CE_{max}$ (cd $A^{-1}$) [b] | $PE_{max}$ (lm $W^{-1}$) [c] | $EQE_{max}$ (%)[d] | Peak (nm) | FWHM (nm)[e] | CIE |
|---|---|---|---|---|---|---|---|
| CzPN | 3.4 | 5.1 | 4.7 | 5.3 | 448 | 72 | (0.15, 0.11) |
| tMCzPN | 3.3 | 65.9 | 62.7 | 26.0 | 500 | 90 | (0.20, 0.42) |

[a] *Turn-on voltage, measured at the luminance of 1 cd* $m^{-1}$. [b] *Maximum current efficiency.* [c] *Maximum power efficiency.* [d] *Maximum external quantum efficiency.* [e] *Full-width at half-maximum.*

tMCzPN both exhibit shapeless fluorescent spectra peaked at 446 and 487 nm, respectively. Due to the stronger electron-donating ability of tMCz, the fluorescence of tMCzPN is evidently red-shifted. At 77 K, we obtained the phosphorescent spectra of two compounds. CzPN showed a local-excited feature phosphorescence with two sharp peaks, because the extended conjugation lowers the triplet energy level of Cz. While tMCzPN exhibits a shapeless and board phosphorescence, suggesting its $T_1$ state is still ICT characteristic. From the peaks of fluorescent and phosphorescent spectra, the $S_1$ and $T_1$ energy levels are estimated to be 2.78 and 2.46 eV for CzPN, and 2.55 and 2.45 eV for tMCzPN. As listed in **Table 1**, the $\Delta E_{ST}$s of CzPN and tMCzPN are estimated to be 0.32 and 0.10 eV, respectively. With a large $\Delta E_{ST}$ and different features of $S_1$ and $T_1$ states, the up-conversion from triplet to singlet excitons will be inhibited, making it difficult for CzPN to possess TADF characteristic. Reversely, the small $\Delta E_{ST}$ of 0.10 eV will lead tMCzPN to realize an efficient RISC process and exhibit TADF behavior. In DPEPO films at room temperature, the PLQYs of CzPN and tMCzPN were measured to be 93.3 and 70.5%, respectively. With a significant overlap between HOMO and LUMO, the fluorescence process of singlet excitons is efficient for CzPN, and it can be an excellent conventional fluorescent emitter. Additionally, tMCzPN also realizes quite a high PQLY for TADF emitters.

To further prove their TADF characteristics, the transient PL decays of the two compounds doped into DPEPO films were measured. In the order of a microsecond, no delayed component was observed for CzPN, indicating its non-TADF characteristic. While for tMCzPN, a delayed decay with a lifetime of 14.29 μs was obtained at room temperature. We also measured the temperature-dependent transient PL decays of the tMCzPN doped DPEPO film from 100 to 300 K. As shown in **Figure 4E**,

the delayed component clearly enhanced with the increasing temperature, due to the acceleration of the up-conversion from triplet to singlet excitons by thermal activation, which directly demonstrated the TADF characteristic of tMCzPN. By replacing the common Cz with tMCz, CzPN, and tMCzPN exhibit significant differences in some key photophysical properties. Thus, compared to Cz, tMCz is more convenient to develop TADF emitters.

### Electroluminescence Properties

To investigate the EL performance of two compounds, devices with structures of ITO/TAPC (35 nm)/TCTA (10 nm)/CzSi (10 nm)/DPEPO: CzPN or tMCzPN (20 wt%) (20 nm)/TmPyPb (40 nm)/LiF (1 nm)/Al were fabricated. Herein, indium tin oxide (ITO) was the anode, 4,4′-cyclohexylidenebis[N,N-bis(4-methylphenyl)aniline (TAPC) and 4,4′,4″-tris(carbazolyl)triphenylamine (TCTA) were the hole-transporting layers, 9-(triphenyl-silyl)-9H-carbazole (CzSi) was the exciton-blocking layer, 1,3,5-tri(m-pyrid-3-yl-phenyl)benzene (TmPyPb) was electron-transporting, hole-blocking, and exciton-blocking layer, LiF was the electron injection layer, and Al was the cathode, respectively. CzPN or tMCzPN doped DPEPO was used as the emitting layers, and the doping concentration was optimized to 20 wt%.

As shown in **Figure 5** and listed in **Table 2**, both devices show close turn on voltages of 3.4 V and 3.3 V, respectively for CzPN and tMCzPN. The similar turn on voltages should be attributed to the use of the same host material, which is consistent with the results of the reported devices using DPEPO as the host. In the devices, CzPN exhibits a stable blue emission with a peak at 448 nm and a CIE coordinate of (0.15, 0.11), while tMCzPN shows a stable cyan emission with a peak at 500 nm and a CIE coordinate of (0.20, 0.42). The red-shift between two EL spectra should be mainly ascribed to the stronger electron-donating ability of tMCz compared with Cz, and is consistent with their PL spectra in DPEPO films. Additionally, from the EL spectra, the full-width at half-maximum is 72 nm for CzPN, evidently narrower than 90 nm for tMCzPN. This is because CzPN has a higher conjugation between the D and A segments, and thereby possesses a stronger molecular restriction to confine structural relaxation. The maximum forward-viewing efficiencies of CzPN-based OLED are 4.7 cd $A^{-1}$ for CE, 4.7 lm $W^{-1}$ for PE, and 5.3% for EQE, respectively. The EQE of 5.3% is consistent with the theoretical limitation of the OLEDs based on traditional fluorescent emitters, demonstrating the non-TADF characteristic of CzPN yet again. Without any light out-coupling enhancement, the tMCzPN-based device exhibits extremely high forward-viewing maximum CE, PE and EQE of 65.9 cd $A^{-1}$, 62.7 lm $W^{-1}$ and 26.0%, respectively. To the best of our knowledge, such a high EQE of 26.0% is among the best performance for TADF-based OLEDs. Thus, by simply replacing common Cz with tMCz, the non-TADF fluorophor CzPN is successfully transformed to an excellent TADF emitter tMCzPN, indicating that tMCz is a more appropriate candidate than Cz, for developing TADF emitters.

## CONCLUSION

Due to the insufficient steric hindrance of Cz, additional groups are generally required to enhance the separation between HOMO and LUMO for Cz-based TADF emitters, resulting in complicated synthetic procedures and high costs. To address this issue, we replaced Cz with its derivative tMCz to develop TADF emitters, and designed and synthesized two novel compounds CzPN and tMCzPN accordingly. With the same and simple molecular framework, two compounds exhibit evident differences due to the additional methyl groups on tMCz. tMCzPN possesses a more twisted molecular structure and successfully realizes the TADF characteristic with a small $\Delta E_{ST}$ of 0.10 eV, while CzPN is a non-TADF fluorophor. In the devices, tMCzPN exhibits an extremely high forward-viewing maximum EQE of 26.0%, without any light out-coupling enhancement, which is significantly higher than that of 5.3% for CzPN. These results indicate that tMCzPN is an excellent TADF emitter and proves that tMCz is a more appropriate candidate than Cz for developing TADF emitters with a simple molecular framework.

## AUTHOR CONTRIBUTIONS

J-LC and WL contributed equally to this work. C-JZ, S-LT, and X-HZ designed whole work. J-LC, WL, and J-XC synthesized the organic compounds. J-LC, KW, and Y-ZS characterize the physical properties of compounds. WL and MZ fabricated and optimized the devices. J-LC and WL wrote the paper with support from C-JZ, S-LT, and X-HZ. All authors contributed to the general discussion.

## ACKNOWLEDGMENTS

This work was supported by the National Natural Science Foundation of China (Grant No. 51773029, 61775029, 51533005, 51373190), the National Key Research & Development Program of China (Grant No. 2016YFB0401002), the Collaborative Innovation Center of Suzhou Nano Science & Technology, the Priority Academic Program Development of Jiangsu Higher Education Institutions (PAPD) and the 111 Project and Qing Lan Project, P. R. China.

## REFERENCES

Adachi, C., Baldo, M. A., Thompson, M. E., and Forrest, S. R. (2001). Nearly 100% internal phosphorescence efficiency in an organic light-emitting device. *J. Appl. Phys.* 90, 5048–5051. doi: 10.1063/1.1409582

Baldo, M. A., O'Brien, D. F., Thompson, M. E., and Forrest, S. R. (1999). Excitonic singlet-triplet ratio in a semiconducting organic thin film. *Phys.Rev.B.* 60, 14422–14428.

Baldo, M. A., O'Brien, D. F., You, Y., Shoustikov, A., Sibley, S., Thompson, M. E., et al. (1998). Highly efficient phosphorescent emission from organic electroluminescent devices. *Nature* 395, 151–154. doi: 10.1038/25954

Chan, C. Y., Cui, L. S., Uk, K. J., Hajime, N., and Chihaya, A. (2018). Efficient and stable sky-blue delayed fluorescence organic light-emitting diodes with CIEy below 0.4. *Adv. Funct. Mater.* 28:1706023. doi: 10.1002/adfm.201706023

Chen, J.-X., Liu, W., Zheng, C. J., Wang, K., Liang, K., Shi, Y. Z., et al. (2017). Coumarin-based thermally activated delayed fluorescence emitters with high external quantum efficiency and low efficiency roll-off in the devices. *ACS APPL. Mater. Interfaces* 9, 8848–8854. doi: 10.1021/acsami.6b15816

Choi, S., Godumala, M., Lee, J. H., Kim, G. H., Moon, J. S., Kim, J. Y., et al. (2017). Optimized structure of silane-core containing host materials for highly efficient blue TADF OLEDs. *J. Mater. Chem. C.* 5, 6570–6577. doi: 10.1039/C7TC01357D

Cui, L.-S., Nomura, H., Geng, Y., Kim, J. U., Nakanotani, H., and Adachi, C. (2017). Controlling singlet–triplet energy splitting for deep-blue thermally activated delayed fluorescence emitters. *Angew. Chem. Int. Ed.* 56,1571–1575. doi: 10.1002/anie.201609459

Endo, A., Ogasawara, M., Takahashi, A., Yokoyama, D., Kato, Y., and Adachi, C. (2009). Thermally activated delayed fluorescence from Sn(4+)-porphyrin complexes and their application to organic light emitting diodes–a novel mechanism for electroluminescence. *Adv. Mater.* 21, 4802–4806. doi: 10.1002/adma.200900983

Endo, A., Sato, K., Yoshimura, K., Kai, T., Kawada, A., Miyazaki, H., et al. (2011). Efficient up-conversion of triplet excitons into a singlet state and its application for organic light emitting diodes. *Appl. Phys. Lett.* 98:083302. doi: 10.1063/1.3558906

Goushi, K., Kou, Y., Sato, K., and Adachi, C. (2012). Organic light-emitting diodes employing efficient reverse intersystem crossing for triplet-to-singlet state conversion. *Nat. Photonics*. 6, 253–258. doi: 10.1038/nphoton.2012.31

Hirata, S., Sakai, Y., Masui, K., Tanaka, H., Lee, S. Y., Nomura, H., et al. (2014). Highly efficient blue electroluminescence based on thermally activated delayed fluorescence. *Nat. Mater.* 14, 330–336. doi: 10.1038/nmat4154

Li, W., Zhao, J., Li, L., Du, X., Fan, C., Zheng, C., et al. (2018). Efficient solution-processed blue and white OLEDs based on a high-triplet bipolar host and a blue TADF emitter. *Org. Electron.* 58, 276. doi: 10.1016/j.orgel.2018.04.027

Liang, J., Li, C., Zhuang, X., Ye, K., Liu, Y., and Wang, Y. (2018). Novel blue bipolar thermally activated delayed fluorescence material as host emitter for high-efficiency hybrid warm-white OLEDs with stable high color-rendering index *Adv. Funct. Mater.* 28:1707002. doi: 10.1002/adfm.201707002

Liu, W., Chen, J. X. Zheng, C. J., Wang, K., Chen, D. Y., Li, F., et al. (2016). Novel strategy to develop exciplex emitters for high-performance OLEDs by employing thermally activated delayed fluorescence materials. *Adv. Funct. Mater.* 26, 2002–2008. doi: 10.1002/adfm.201505014

Liu, W., Chen, Z., Zheng, C. J., Liu, X. K., Wang, K., Li, F., et al. (2015b). A novel nicotinonitrile derivative as an excellent multifunctional blue fluorophore for highly efficient hybrid white organic light-emitting devices. *J. Mater. Chem. C.* 3, 8817–8823. doi: 10.1039/C5TC01415H

Liu, W., Zheng, C. J., Wang, K., Chen, Z., Chen, D. Y., Li, F., et al. (2015a). Novel carbazol-pyridine-carbonitrile derivative as excellent blue thermally activated delayed fluorescence emitter for highly efficient organic light-emitting devices. *ACS Appl. Mater. Interfaces*. 7, 18930–18936. doi: 10.1021/acsami.5b05648

Liu, X. K., Zhan, C., Zheng, C. J., Liu, C. L., Lee, C. S., Li, F., et al. (2015c). Prediction and design of efficient exciplex emitters for high-efficiency, thermally activated delayed-fluorescence organic light-emitting diodes. *Adv. Mater.* 27, 2378–2383. doi: 10.1002/adma.201405062

Méhes, G., Nomura, H., Zhang, Q., Nakagawa, T., and Adachi, C. (2012). Enhanced electroluminescence efficiency in a spiro-acridine derivative through thermally activated delayed fluorescence. *Angew. Chem. Int. Ed.* 51, 11311–11315. doi: 10.1002/anie.201206289

Mounggon, K., Kyu, J. S., Seok-Ho, H., and Yeob, L. J. (2015). Stable blue thermally activated delayed fluorescent organic light-emitting diodes with three times longer lifetime than phosphorescent organic light-emitting diodes. *Adv. Mater.* 27, 2515–2520. doi: 10.1002/adma.201500267

Okamoto, S., Tanaka, K., Izumi, Y., Adachi, H., Yamaji, T., and Suzuki, T. (2001). Simple measurement of quantum efficiency in organic electroluminescent devices*Jpn. J. Appl. Phys.* 40, 783–784. doi: 10.1143/JJAP.40.L783

Pashazadeh, R., Pander, P., Lazauskas, A., Dias, F. B., and Grazulevicius, J. V. (2018). Multicolor luminescence switching and controllable thermally activated delayed fluorescence turn on/turn off in carbazole–quinoxaline–carbazole triads. *J. Phys. Chem. Lett.* 9, 1172–1177. doi: 10.1021/acs.jpclett.8b00136

Peng, Q., Li, W., Zhang, S., Chen, P., Li, F., and Ma, Y. (2013). Evidence of the reverse intersystem crossing in intra-molecular charge transfer flourenscene based organic light-emmitting devices through magneto-electroluminescene measurements. *Adv. Opt. Mater.* 1, 362–366. doi: 10.1002/adom.201300028

Pope, M., Kallmann, H. P., and Magnante, P. (1963). Electroluminescence in Organic Crystals. *J. Chem. Phys.* 38, 2042–2043. doi: 10.1063/1.1733929

Rajamalli, P., Thangaraji, V., Senthilkumar, N., Ren-Wu, C. C. Lin, H. W., and Cheng, C. H. (2017). Thermally activated delayed fluorescence emitters with a *m*,*m*-di-*tert*-butyl-carbazolyl benzoylpyridine core achieving extremely high blue electroluminescence efficiencies *J. Mater. Chem. C.* 5, 2919–2926. doi: 10.1039/C7TC00457E

Sajoto, T., Djurovich, P. I., Tamayo, A. B., Oxgaard, J., Goddard, W. A. III, and Thompson, M. E. (2009). Temperature dependence of blue phosphorescent cyclometalated Ir(III) complexes. *J. Am. Chem. Soc.* 131, 9813–9822. doi: 10.1021/ja903317w

Segal, M., Baldo, M. A., Holmes, R. J., Forrest, S. R., and Soos, Z. G. (2003). Excitonic singlet-triplet ratios in molecular and polymeric organic materials. *PhRvB*. 68, 338–344. doi: 10.1103/PhysRevB.68.075211

Shi, Y. Z., Wang, K., Li, X., Dai, G. L., Liu, W., Ke, K., et al. (2018). Intermolecular charge-transfer transition emitter showing thermally activated delayed fluorescence for efficient non-doped OLEDs. *Angew. Chem. Int. Ed.* 57:9480. doi: 10.1002/anie.201804483

Tang, C. W., and VanSlyke, S. A. (1987). Organic electroluminescent diodes. *Appl. Phys. Lett.* 51, 913–915. doi: 10.1063/1.98799

Uoyama, H., Goushi, K., Shizu, K., Nomura, H., and Adachi, C. (2012). Highly efficient organic light-emitting diodes from delayed fluorescence. *Nature* 492, 234–238. doi: 10.1038/nature11687

Wang, K., Zheng, C. J., Liu, W., Liang, K., Shi, Y. Z., Tao, S. L., et al. (2017). Avoiding energy loss on TADF emitters: controlling the dual conformations of D-A structure molecules based on the pseudoplanar segments. *Adv. Mater.* 29:1701476. doi: 10.1002/adma.201701476

Yersin, H., Rausch, A. F., Czerwieniec, R., Hofbeck, T., and Fischer, T. (2011). The triplet state of organo-transition metal compounds. Triplet harvesting and singlet harvesting for efficient OLEDs. *Coord. Chem. Rev.* 255, 2622–2652. doi: 10.1016/j.ccr.2011.01.042

Zhang, D., Duan, L., Li, C., Li, Y., Li, H., Zhang, D., et al. (2014a). High-efficiency fluorescent organic light-emitting devices using sensitizing hosts with a small singlet-triplet exchange energy. *Adv. Mater.* 26, 5050–5055. doi: 10.1002/adma.201401476

Zhang, D., Song, X., Cai, M., Kaji, H., and Duan, L. (2018). Versatile indolocarbazole-isomer derivatives as highly emissive emitters and ideal hosts for thermally activated delayed fluorescent OLEDs with alleviated efficiency roll-off. *Adv. Mater.* 30:1705406. doi: 10.1002/adma.201705406

Zhang, D., Wei, P., Zhang, D., and Duan, L. (2017). Sterically shielded electron transporting material with nearly 100% internal quantum efficiency and long lifetime for thermally activated delayed fluorescent and phosphorescent OLEDs. *ACS Appl. Mater. Interfaces.* 9, 19040–19047. doi: 10.1021/acsami.7b04391

Zhang, Q., Kuwabara, H., Potscavage, W. J., Huang, S., Hatae, Y., Shibata, T., et al. (2014b). Anthraquinone-based intramolecular charge-transfer compounds: computational molecular design, thermally activated delayed fluorescence, and highly efficient red electroluminescence. *J. Am. Chem. Soc.* 136, 18070–18081. doi: 10.1021/ja510144h

Zhang, Q., Li, B., Huang, S., Nomura, H., Tanaka, H., and Adachi, C. (2014c). Efficient blue organic light-emitting diodes employing thermally activated delayed fluorescence. *Nat. Photonics*. 8, 326–332. doi: 10.1038/nphoton.2014.12

Zhang, Q., Li, J., Shizu, K., Huang, S., Hirata, S., Miyazaki, H., et al. (2012). Design of efficient thermally activated delayed fluorescence materials for pure blue organic light emitting diodes. *J. Am. Chem. Soc.* 134, 14706–14709. doi: 10.1021/ja306538w

Zhang, S., Yao, L., Peng, Q., Li, W., Pan, Y., Xiao, R., et al. (2015). Achieving a significantly increased efficiency in nondoped pure blue fluorescent OLED: a quasi-equivalent hybridized excited state. *Adv. Funct. Mater.* 25, 1755–1762. doi: 10.1002/adfm.201404260

Zheng, C. J., Wang, J., Ye, J., Lo, M. F., Liu, X. K., Fung, M. K., et al. (2013). Novel efficient blue fluorophors with small singlet-triplet splitting: Hosts for highly efficient fluorescence and phosphorescence hybrid WOLEDs with simplified structure. *Adv. Mater.* 25, 2205–2211. doi: 10.1002/adma.201204724

**Conflict of Interest Statement:** The authors declare that the research was conducted in the absence of any commercial or financial relationships that could be construed as a potential conflict of interest.